Illustration of HIV-1 Protease Folding through a Molten-Globule-like Intermediate Using an Experimental Model that Implicates α-Crystallin and Calcium Ions

Chandravanu Dash,[‡,§] Murali Sastry,[||] and Mala Rao*[,§]

Biochemical and Material Sciences Division, National Chemical Laboratory, Pune-411 008, India

Received July 29, 2004; Revised Manuscript Received November 28, 2004

ABSTRACT: The folding of HIV-1 protease to its active form involves the coordination of structure formation and dimerization, which follows a hierarchy consisting of folding nuclei spanning from the active site, hinge region, and dimerization domain. However, the biochemical characteristics of the folding intermediates of this protein remain to be elucidated. In an experimental model, the denaturation of the tethered dimer of HIV-1 protease by guanidine hydrochloride revealed an alternative conformation resembling the molten-globule state. The molten-globule state binds to the molecular chaperone α-crystallin and prevents its aggregation; however, the chaperone alone failed to reconstitute HIV-1 protease into its active form. Calcium ion assisted in the release of active enzyme from the chaperone complex. α-crystallin, a member of the small heat-shock protein, assists proteins to fold correctly; however, the underlying principle of signals responsible for chaperone-mediated protein folding remains enigmatic. X-ray photoelectron spectroscopy has been employed to provide the evidence of calcium binding to α-crystallin and to decipher the effect of calcium binding on the chaperone-mediated refolding of HIV-1 protease. On the basis of our spectroscopic data, we propose that calcium ions interact with the carboxyl groups of the surface-exposed acidic amino acids of α-crystallin bringing electrostatic interference, which plays a pivotal role in inducing conformational changes in the chaperone responsible for the release of the active enzyme.

Elucidating the mechanistic details underlying the efficient refolding of proteins is an important consideration for defining how proteins fold to their native structure. The structural stability of a protein is a delicate balance between the native conformation that may be considered unique, persistent, and stable and the random-coil state, which is a dynamic ensemble of highly flexible irregular structures. It has been assumed for a long time that protein folding in cells occurs spontaneously, except for organellar-exported proteins that require a cellular targeting and translocation machinery to reach their destination. This concept has been challenged by the discovery of a cellular network of molecular chaperones and folding catalysts that assist in folding processes in virtually all compartments (*1*, *2*). The major classes of chaperones are the Hsp40, Hsp60, Hsp70, Hsp90, Hsp100, and small heat-shock proteins (sHsps)[1] (*3*). sHsps represent an abundant family of stress proteins present in virtually all types of organisms, and the abundance of sHsps under physiological conditions varies significantly on the cell type and organism (*4*−*6*). Under heat-shock conditions, the level of sHsps increases drastically, amounting up to 1% of the total cellular protein (*7*), suggesting functional importance in survival at higher temperatures. The eye lens protein α-crystallin is a member of the sHsp family because of its similar structural and functional properties (*8*−*11*). α-Crystallin suppresses aggregation of damaged proteins and plays a crucial role in maintaining the transparency of the ocular lens, and the failure of this function could contribute to the development of cataracts (*12*, *13*). sHsps were also shown to suppress aggregation of unfolded proteins and increase the yield of reactivation of denatured substrate proteins (*14*−*16*), and there are reports suggesting the role of ATP in α-crystallin-mediated refolding of the substrate protein (*17*−*19*). However, little is known about the molecular mechanism of these chaperones and their integration into the chaperone system of the cell. Very recently, the structural changes in α-crystallin have been reported, and also the quaternary structure of α-crystallin has been shown to be necessary for its chaperone-like activity (*20*, *21*). Along with α-crystallin, calcium ions (Ca^{2+}), the second messenger of eukaryotic cells, also play a major role in the physiology of cataract formation. The effects of endogenous calcium on lens transparency involve several factors including aggregation of the lens proteins crystallins at high Ca^{2+} concentrations (*22*, *23*). Although the cytotoxic effects of internal calcium on lens physiology have been established, there has not been much attention toward the interaction of Ca^{2+} and α-crystallin and its correlation to the protection of proteins under stress conditions. Recent reports on the effect of

* To whom correspondence should be addressed. Telephone: 91-20-589 3034. Fax: 91-20-588 4032. E-mail: malarao@dalton.ncl.res.in.

‡ Current address: Resistance Mechanisms Laboratory, HIV Drug Resistance Program, National Cancer Institute, Frederick, MD 21702.

§ Biochemical Science Division.

|| Material Science Division.

[1] Abbreviations: HIV, human immunodeficiency virus; sHsp, small heat-shock protein; PR, protease; MG, molten globule; GdnHCl, guanidine hydrochloride; XPS, X-ray photoelectron spectroscopy; BE, binding energy; ANS, 8-anilinonaphthalene-1-sulfonic acid; AIDS, acquired immunodeficiency syndrome; CD, circular dichroism; NMR, nuclear magnetic resonance; TFR, transframe region; TFP, transframe octapeptide; RT, reverse transcriptase; SDS−PAGE, sodium dodecyl sulfate−polyacrylamide gel electrophoresis.

10.1021/bi048378n CCC: $30.25
Published on Web 02/17/2005

calcium ions on the thermal stability of α-crystallin have shed some light on the correlation of the chaperone and metal ion functions (*24*, *25*).

The essential role of human immunodeficiency virus (HIV)-1 protease (PR) in virion maturation makes this enzyme an important therapeutic target for the treatment of acquired immunodeficiency syndrome (AIDS) (*26*). The PR catalyzes its own release from the Gag-Pol polyprotein in addition to the maturation of the virally encoded structural proteins and enzymes required for the assembly and production of viable virions. The autoprocessing of the virus-encoded Gag and Gag-Pol polyproteins is one of the essential steps in the life cycle of HIV-1. This cleavage of viral precursors yields the functional, structural, and catalytic viral proteins needed for virus maturation and efficient infection. The functional PR is a 22-kDa homodimer that self-assembles from two identical pylopeptide chains of 99 residues. Extensive nuclear magnetic resonance (NMR) structural and dynamic studies have been reported on the folded protein complexed to different inhibitors (*27*−*29*). Characterization of partially folded/unfolded states created by denaturants can provide useful insights into the structural features of the kinetic intermediates. Recently, systematic monitoring of the hierarchy of folding propensities of HIV-1 PR by NMR analysis (*30*, *31*) and by molecular simulations has been reported (*32*). However, a detailed biochemical analysis of the folding intermediates has not been undertaken. In this report, we have attempted to decipher the folding pathway of HIV-1 PR in detail and also addressed the correlation of chaperone function of α-crystallin and Ca^{2+} using this enzyme in an experimental system. For the first time, we provide the direct evidence of a molten-globule (MG) state in the folding pathway of HIV-1 PR, which was protected from aggregation by α-crystallin. Structural and functional implications of Ca^{2+} binding to the α-crystallin−MG complex served to implicate the proposed correlation between the metal ion and the chaperone function of α-crystallin.

MATERIALS AND METHODS

Materials. Pure α-crystallin, Lys-Ala-Arg-Val-Nle-*p*-nitro-Phe-Glu-Ala-Nle-amide, and bovine serum albumin (BSA) were obtained from Sigma Co. All other chemicals are of analytical grade.

Purification of HIV-1 PR and Enzymatic Assay. The *Escherichia coli* MC1061 containing plasmid pPTΔN containing the recombinant HIV-1 PR that was grown in M9 medium supplemented with 0.2% casamino acids and 50 μg/mL ampicillin. After the onset of the log phase of bacterial growth, the temperature was shifted to 42 °C for 60 min and the bacteria were then pelleted. HIV-1 PR was purified as previously reported (*33*). Briefly, the bacteria were lysed by sonication and centrifuged at 27000*g* for 30 min. The protein was purified by ammonium sulfate precipitation, dialysis, and gel-filtration chromatography and stored at −80 °C in the presence of 10% glycerol. The HIV-1 PR activity was assayed using the synthetic substrate Lys-Ala-Arg-Val-Nle-*p*-nitro-Phe-Glu-Ala-Nle-amide. The HIV-1 PR was incubated at 37 °C with the substrate in a reaction mixture containing 100 mM NaCl, 5 mM β-mercaptoethanol, 5 mM ethylenediaminetetraacetic acid (EDTA), and 50 mM sodium acetate buffer at pH 5.6. After 15 min, the reaction was stopped by the addition of an equal volume of 5% trichloroacetate and followed by incubation for 30 min at 28 °C. The cleavage products were analyzed by RP-HPLC and by a decrease in absorbance at 300 nm (*33*).

Denaturation and Renaturation of HIV-1 PR. All experiments described below were performed in the presence of 50 mM sodium phosphate buffer at pH 6.0. For unfolding studies, 100 μM of purified HIV-1 PR was incubated with increasing concentrations of GdnHCl (1−8 M) for 2 h at 28 °C. Renaturation was initiated by diluting 10 μL of the sample into 1 mL of buffer and was mixed for 6−8 h at 28 °C. For the chaperone-assisted refolding, α-crystallin was added at different molar concentrations in the reaction mixture containing 1 μM of HIV-1 PR. $CaCl_2$ or $MgCl_2$ was added at 5 mM to the complexed α-crystallin−HIV-1 PR. As a control, $MgCl_2$ was also added at 5 mM to the complexed α-crystallin−HIV-1 PR. Aliquots (100 μL) were withdrawn at various times of refolding and assayed for proteolytic activity of HIV-1 PR. Reactivation of chemically denatured HIV-1 PR was calculated as the percentage activity relative to a control sample of native HIV-1 PR tested under identical conditions. Additional experimental details are provided in the figure captions. As a control experiment, BSA was added to the renaturation buffer at different molar concentrations to test its ability to refold the unfolded HIV-1 PR.

Fluorescence and Circular Dichroism (CD) Analysis. Fluorescence measurements were performed on a Perkin−Elmer LS50 Luminescence spectrometer. Protein fluorescence was excited at 295 nm, and the emission was recorded in 0.05 M phosphate buffer in the absence or presence of guanidine hydrochloride (GdnHCl) from 300 to 500 nm at 25 °C. The slit widths on both the excitation and emission were set at 5 nm, and the spectra were obtained at 500 nm/min. Fluorescence data were the average of 6 scans with the baseline corrected by an appropriate buffer control. For titration analysis, $CaCl_2$ was added to α-crystallin at different concentrations and the stoichiometry was measured by fluorescence.

CD spectra of HIV-1 PR were recorded in a Jasco-J715 spectropolarimeter at ambient temperature using a cell of 1 mm path length. Replicate scans were obtained at 0.1 nm resolution, 0.1 nm bandwidth, and a scan speed of 50 nm/min in 50 mM sodium phosphate buffer (pH 6.0) in the absence or presence of increasing concentrations of GdnHCl. Spectra were the average of 6 scans with the baseline subtracted spanning from 350 to 200 nm.

8-Anilinonaphthalene-1-sulfonic Acid (ANS) Binding and Aggregation Assay. The GdnHCl-treated HIV-1 PR was incubated with a 2-fold molar excess of ANS for 1 h in the dark. The ANS fluorescence was recorded with an excitation at 375 nm and an emission in the range of 400−600 nm, with the slit widths on both the excitation and emission set at 5 nm and a scan speed of 100 nm/min.

To monitor aggregation of the unfolded HIV-1 PR, light scattering was measured in a Perkin−Elmer luminescence spectrophotometer in stirred and thermostated quartz cells. Time course of the protein fluorescence was measured with the excitation and emission wavelengths fixed at 375 nm. Background buffer spectra were subtracted to remove the contribution from Raman scattering.

Gel-Filtration Chromatography. All size-exclusion chromatography was carried out using a 10 × 300 mm Superose-6 column (Amersham Biosciences). A total of 0.1 mL of samples of protein was centrifuged for 5 min at 14000*g* before application. Chromatography was carried out at 25 °C in 50 mM sodium phosphate buffer (pH 6.0) with a flow rate of 0.25 mL/min. The absorbance was monitored at a wavelength of 280 nm. Protein fractions were collected manually, pooled, concentrated, and analyzed by sodium dodecyl sulfate−polyacrylamide gel electrophoresis (SDS−PAGE).

X-ray Photoelectron Spectroscopy (XPS) Analysis. XPS measurements on the drop-coated protein films were carried out on a VG MicroTech ESCA 3000 instrument at a pressure better than 1×10^{-9} Torr. All of the photoemission spectra were recorded with unmonochromatized Mg Kα radiation (photon energy = 1253.6 eV) at a pass energy of 50 eV and electron takeoff angle (angle between the electron emission direction and surface plane) of 60°. The overall resolution was ∼1 eV for the XPS measurements. After the general scan spectra were recorded, the C 1s, Ca 2p, and N 1s core levels were recorded at a high signal-to-noise ratio. The core level spectra were background-corrected using the Shirley algorithm (*50*), and the chemically distinct species were resolved using a nonlinear least-squares procedure. The core level binding energies (BEs) were aligned by taking the adventitious carbon BE as 285 eV. The samples are prepared at concentrations similar to that mentioned for the refolding experiments.

RESULTS

HIV-1 PR Unfolds through a MG State. For the unfolding studies, HIV-1 PR was incubated with increasing concentrations (1−8 M) of GdnHCl, and the changes induced in the secondary and tertiary structures of the enzyme were monitored by various spectroscopic methods. The fluorescence of the surface-exposed Trp residues has been used as a probe for monitoring the changes in the tertiary structure of the protein (*33*). The native HIV-1 PR has an emission maxima (λ_{max}) at 340 nm as a result of the radiative decay of the $\pi - \pi^*$ transition from the Trp residues. When HIV-1 PR was treated with 1−3 M GdnHCl, a pronounced red shift in the λ_{max} was observed (Figure 1); however, there was a minimal shift in λ_{max} at 4−8 M GdnHCl, indicating exposure of the tryptophan residues as a consequence of the successive unfolding of the protein. Figure 2 depicts the CD spectra of the HIV-1 PR at different concentrations of GdnHCl. At 2 M GdnHCl, the mean residue ellipticity of HIV-1 PR at 220 nm was decreased by almost 50%; however, at increased denaturant concentrations, there was further reduction of negative ellipticity, until the substantial loss and collapse of the secondary structure at 8 M GdnHCl (Figure 2A). The near- and far-UV CD spectra of HIV-1 PR in 1−3 M concentrations of GdnHCl are shown in Figure 2B. The far-UV CD spectra of the HIV-1 PR treated with GdnHCl at 1−3 M revealed the changes in the structure of the protein, indicating formation of partly folded species during the unfolding process. These results corroborated the presence of partly folded structures of HIV-1 PR at lower denaturant concentrations previously described by Bhavesh et al. The near-UV CD spectra revealed that, at 1 M GdnHCl, the spectrum shows some decrease in the ellipticity, whereas at

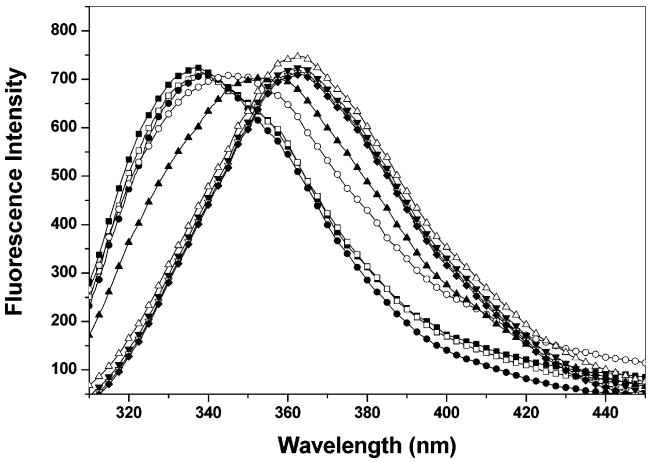

FIGURE 1: Fluorescence analysis of the unfolding of HIV-1 PR. HIV-1 PR (100 μM) was treated with the denaturant in 50 mM sodium phosphate buffer at pH 6.0. Trp fluorescence was excited at 295 nm, and the emission was measured from 300 to 450 nm. The native protein (■) was treated with GdnHCl at concentrations of 1 (□), 2 (●), 3 (○), 4 (▲), 5 (△), 6 (▼), 7 (▽), and 8 M (◆).

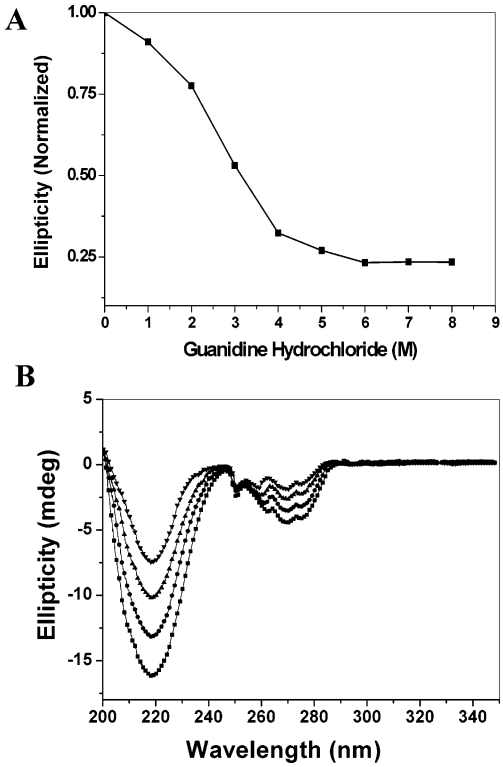

FIGURE 2: CD analysis of the unfolding of HIV-1 PR. HIV-1 PR (100 μM) was treated with GdnHCl from 0 to 8 M concentrations in 50 mM sodium acetate buffer at pH 6.0, and the structural changes of HIV-1 PR were monitored by CD. (A) Mean residue ellipticity at 220 nm of the GdnHCl-treated HIV-1 PR. (B) Far-UV CD spectra and (C) near-UV spectra of the HIV-1 PR treated with GdnHCl at concentrations of 0 (■), 1 (●), 2 (▲), and 3 M (▼).

2M GdnHCl, the protein exhibits highly decreased ellipticity, suggesting that the intermediate exhibits substantially loosened side-chain packing, whereas the tertiary structure is substantially lost in 3 M GdnHCl.

To investigate these partly folded structures, we have employed the fluorophore ANS, which specifically binds to the exposed hydrophobic pockets of the partly folded proteins. ANS does not possess fluorescence in aqueous

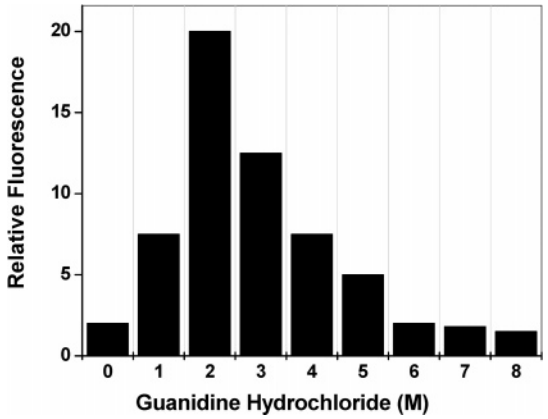

FIGURE 3: Exposure of the hydrophobic surfaces of GdnHCl-treated HIV-1 PR by ANS fluorescence. HIV-1 PR (100 μM) was treated with 0−8 M GdnHCl for 2 h at 28 °C, and the relative exposure of the hydrophobic surface was monitored by ANS fluorescence. A total of 10 μL of the sample was diluted into 1 mL of buffer containing ANS (2 μM) followed by incubation in the dark for 1 h. Fluorescence of the ANS-bound partly/completely unfolded protein was monitored at excitation and emission wavelengths of 375 and 400−600 nm, respectively.

solution; however, upon binding to hydrophobic pockets of proteins, its emission intensity increases with the maximum shifts to shorter wavelengths. Binding of ANS to the 2 M GdnHCl-treated HIV-1 PR resulted in the maximum increase in its fluorescence and also a blue shift to 475 nm, indicating the optimum exposure of the hydrophobic surface of the folding intermediate (Figure 3). The subsequent decrease in the ANS fluorescence of the denatured protein with an increased concentration of GdnHCl indicated a progressive unfolding process. The ANS fluorescence of the native and totally unfolded protein indicated no or minimal binding of the fluorophore. The time-dependent analysis of the ANS fluorescence revealed that at 2 M GdnHCl concentration there was a decrease in the fluorescence as a function of time (data not shown), which could be explained by the tendency of the partially unfolded protein to aggregate. It was evident from the fluorescence and CD studies that, at 2 M GdnHCl, HIV-1 PR retains substantial secondary structure, although the tertiary structure was labile. Altogether, our spectroscopic and ANS-binding studies provided the direct evidence that at 2 M GdnHCl HIV-1 PR partially unfolded to an alternative conformation resembling the MG state, which is a kinetic intermediate.

MG State of the HIV-1 PR Binds to α*-Crystallin.* To refold the completely denatured HIV-1 PR (treated with 8 M GdnHCl), the protein was diluted, dialyzed, and allowed to refold in a renaturation buffer. However, the unfolded protein did not refold to its functional state as revealed by activity measurements (Figure 4). Similar results were also obtained for denatured HIV-1 PR with 2−7 M GdnHCl, which is attributed to the ability of unfolded or partly folded HIV-1 PR to aggregate and was confirmed by light-scattering analysis. Further, to test the probable role of chaperones in the refolding of HIV-1 PR, the unfolded HIV-1 PR was allowed to refold in the presence of the molecular chaperone α-crystallin. An addition of up to 10 M excess of α-crystallin to unfolded HIV-1 PR (at 3−8 M GdnHCl) failed to prevent aggregation; however, the chaperone trapped the HIV-1 PR−MG state at a 1:5 molar ratio and suppressed its aggregation as demonstrated by the light-scattering experiments (Figure 5). The aggregation of the HIV-1 PR−MG decreased as a function of the increased concentration of α-crystallin, indicating the mass-action effects, whereas increasing the concentration of α-crystallin would increase the collisional frequency to favor the formation of the α-crystallin−HIV-1 PR−MG complex as opposed to the formation of the non-native protein aggregates. At lower concentrations, the chaperone could not suppress the aggregation of the MG state completely, indicating the 1:5 ratio as the critical concentration for the rescue of HIV-1 PR−MG (Figure 5).

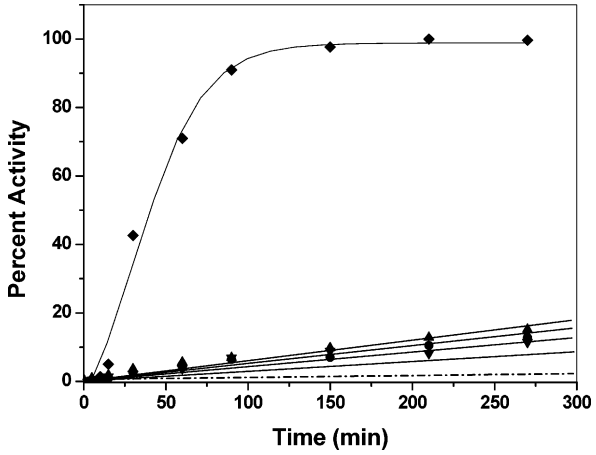

FIGURE 4: Reconstitution of unfolded HIV-1 PR and the regain of enzymatic activity. The proteolytic activity of HIV-1 PR was estimated at 37 °C in a reaction mixture containing 100 mM NaCl, 5 mM β-mercaptoethanol, 5 mM EDTA, and 50 mM sodium acetate buffer at pH 5.6. The HIV-1 PR−MG (■), HIV-1 PR−MG−α-crystallin complex (●), and addition of calcium to the HIV-1 PR−MG (▲) showed no enzymatic activity. Addition of calcium to the HIV-1 PR−MG−α-crystallin complex (◆) resulted in the recovery of the proteolytic activity, indicating the release of the functional protein. Control experiments with addition of 5 mM Mg^{2+} (▼) to the HIV-1 PR−MG−α-crystallin complex and refolding of HIV-1 PR in the presence of BSA and Ca^{2+} (−•−•) did not result in the recovery the enzymatic activity.

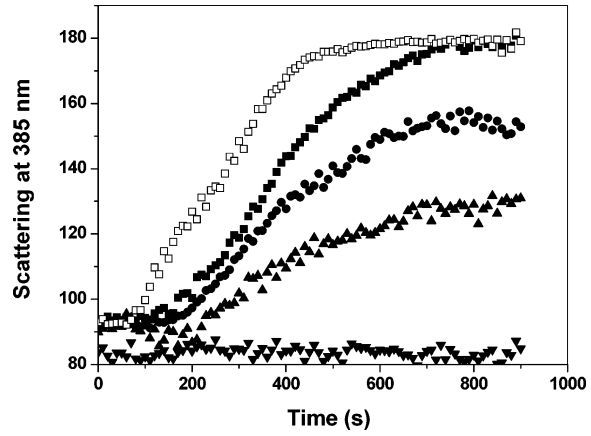

FIGURE 5: Light-scattering assay for the determination of aggregation of HIV-1 PR−MG. The 2 M GdnHCl-treated HIV-1 PR (MG state) and its ability to aggregate were monitored by light scattering at excitation and emission wavelengths of 375 nm. HIV-1 PR−MG at 100 (■) and 200 μM (□) aggregates rapidly when diluted 100-fold because of the interaction of the exposed hydrophobic surface. However, at molar ratios 1:1 (●) and 1:2 (▲) of α-crystallin, the aggregation decreased, whereas at 1:5 molar ratio of α-crystallin (▼), the protein was completely rescued from aggregation, because of the binding of the chaperone to the exposed hydrophobic surface.

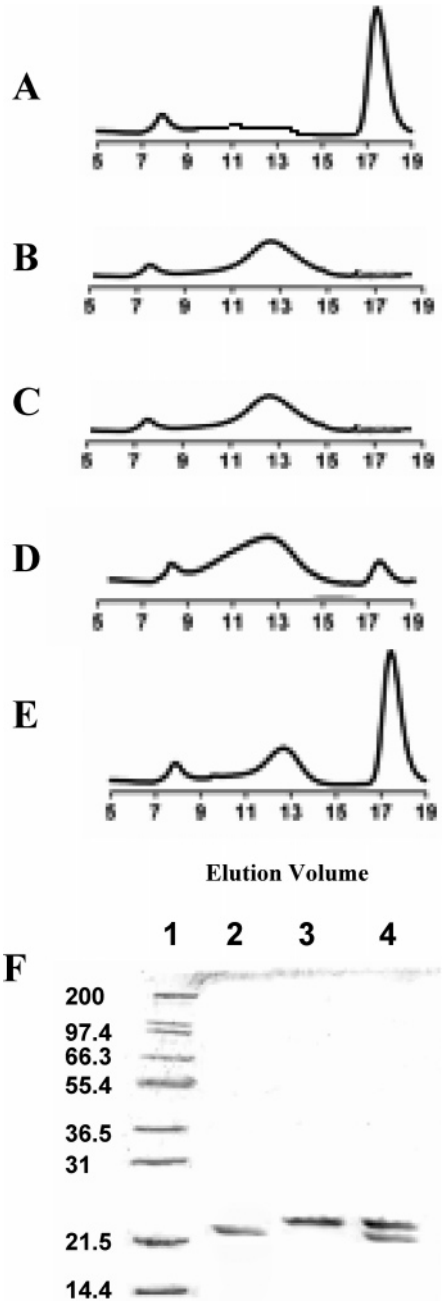

FIGURE 6: Chromatographic analysis of α-crystallin and HIV-1 PR−MG interaction. Gel-filtration chromatography was carried out using a 10 × 300 mm Superose-6 column at 25 °C in 50 mM sodium phosphate buffer (pH 6.0) with a flow rate of 0.25 mL/min. A total of 0.1 mL of samples of protein were centrifuged for 5 min at 14000*g* before application, and the absorbance was monitored at a wavelength of 280 nm. The elution profile of (A) HIV-1 PR−MG, (B) α-crystallin, (C) α-crystallin containing 5 mM $CaCl_2$, (D) the α-crystallin−HIV-1 PR−MG complex, and (E) the α-crystallin−HIV-1 PR−MG complex after addition of $CaCl_2$. (F) SDS−PAGE analysis of the eluents. The eluent from the size-exclusion column was collected, pooled, and concentrated prior to analysis on 12% (w/v) SDS−PAGE. Lane 1, standard molecular weight markers in kilodaltons; lane 2, fraction corresponding to 18 mL peak of HIV-1 PR−MG profile; lane 3, fraction corresponding to 13 mL peak of α-crystallin profile; and lane 4, fraction corresponding to 13 mL peak of the α-crystallin−HIV-1 PR−MG complex profile.

Further, the refolding of HIV-1 PR−MG was initiated in the presence of α-crystallin, wherein aliquots removed at different time intervals were checked for the recovery of enzymatic activity. In the presence of α-crystallin, the enzyme recovered 8% activity (similar to that in the absence of chaperone) after 3 h, although there was no measurable activity up to 30 min (Figure 4). A concomitant decrease in the ability of α-crystallin to bind to HIV-1 PR−MG was observed as a function of time between the dilution of HIV-1 PR−MG and the addition of α-crystallin, which indicated that the chaperone cannot rescue the enzyme once the aggregates are formed. At a higher concentration (200 μM) of the enzyme, the rate of aggregation of the denatured HIV-1 PR was faster as revealed by light scattering (Figure 5). It was observed that unlike α-crystallin, BSA failed to prevent aggregation and mediate the reconstitution of active HIV-1 PR.

Ca^{2+} Binds to the Chaperone−Substrate Complex and Induces Conformational Changes Essential for the Release of the Active Enzyme. Because the refolding of the HIV-1 PR−MG in the absence or presence of α-crystallin did not yield a functional protein, we have tried to refold the protein from the chaperone complex in the presence of the divalent ion calcium. The role of Ca^{2+} ion on the refolding of HIV-1 PR was investigated by adding the metal ion sequentially to the uncomplexed and complexed forms of the protein with the chaperone. When calcium was added to the reaction mixture before the formation of the chaperone−substrate complex, it could not facilitate the reconstitution of the enzyme. However, when the metal ion was added after the formation of the complex, the active enzyme was released from the complex (Figure 4). Control experiments performed in the presence of BSA and Ca^{2+} ion without α-crystallin during refolding did not result in the reconstitution of the active enzyme (Figure 4).

Size-exclusion chromatography has been employed to monitor the complex formation between the α-crystallin and HIV-1 PR−MG and also the release of the substrate protein from the chaperone complex. In Figure 6A, the peak at the elution volume of 18 mL corresponds to the HIV-1 PR−MG, whereas in Figure 6B, the peak at 13 mL represents the elution of the α-crystallin. In the presence of 5 mM $CaCl_2$, the elution profile of α-crystallin remained unchanged (Figure 6C), clearly negating any gross conformational change in the chaperone induced by the metal ion. Figure 6D represents the elution profile of the α-crystallin−HIV-1 PR−MG complex, which revealed that in the complexed form the peak corresponding to HIV-1 PR−MG reduces in size concomitant with the appearance of a broader peak at 13 mL, representing the chaperone−substrate complex. SDS−PAGE analysis of this fraction revealed that it contained both HIV-1 PR and α-crystallin (Figure 6F), which not only confirmed the formation of the chaperone−substrate complex but also indicated that the loss of the HIV-1 PR peak was not a consequences of the formation of aggregates. Figure 6E represents the elution profile of the sample containing the α-crystallin−HIV-1 PR−MG complex, which was incubated with Ca^{2+}. The appearance of both the peaks eluting at 13 and 18 mL, indicated that HIV-1 PR was

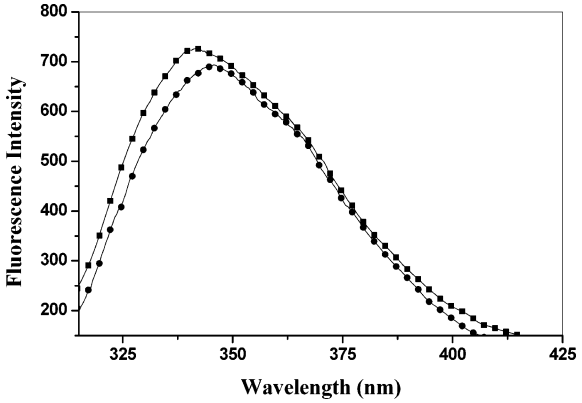

FIGURE 7: Induction of conformational changes in α-crystallin by Ca^{2+}. The intrinsic Trp fluorescence of α-crystallin (■) showed an emission maximum at 340 nm when excited at 295 nm. When $CaCl_2$ (5 mM) was added to the reaction mixture (●), there was a decrease in the emission maximum concomitant with a 3 nm shift.

released from the chaperone complex because of the interaction of the metal ion.

These results revealed the role of Ca^{2+} binding on the release of the protein specifically from the chaperone fundamentally by the induction conformational changes in the complex. To confirm the induction of conformational changes induced in the chaperone because of the metal ion binding, we have carried out fluorescence experiments of α-crystallin and the α-crystallin−HIV-1 PR−MG complex. Upon addition of Ca^{2+}, there was reduction in the quantum yield of Trp fluorescence of α-crystallin concomitant with a shift in the emission maximum (Figure 7). Quenching of the fluorescence can be correlated to the changes in the microenvironment of the Trp residues, whereas the red shift is a consequence of the gross conformational changes induced in the protein by the binding of the metal ion. Our findings on the effect of Ca^{2+} binding on α-crystallin corroborated the results previously reported by Devyani et al. Similar fluorescence results were also obtained for the α-crystallin−HIV-1 PR−MG complex upon addition of Ca^{2+} ions, indicating the conformational changes as a consequence of Ca^{2+} binding to the chaperone (data not shown). The stoichiometric analysis of the metal ion binding to the chaperone revealed an approximate molar ratio of 1:4 per subunit determined by fluorescence. Control experiments with the HIV-1 PR revealed that Ca^{2+} does not bind to the enzyme and does not prevent the HIV-1 PR−MG from aggregation. Use of other divalent cation such as Mg^{2+} failed to assist the reconstitution of the active enzyme in the presence of α-crystallin (Figure 4).

To decipher the functional implications of calcium binding and the conformational changes induced in the α-crystallin−HIV-1 PR−MG complex leading toward the release of active enzyme, XPS analysis has been carried out. XPS provides a direct measurement of the interaction between molecules at the electronic level. Because Ca^{2+} does not bind to HIV-1 PR, the structural changes involved because of binding of the metal ion derived from XPS analysis are assigned to the chaperone−substrate complex. The chaperone−substrate complex used in XPS analysis was prepared at similar conditions and concentrations. Figure 8 shows the XPS spectra indicating the BE in electronvolts of the electrons of C 1s, N 1s, and Ca 2p core levels of the chaperone−substrate complex after background corrections. The C 1s core level spectrum (Figure 8A) in the absence of Ca^{2+} showed two main peaks centered at BEs of 285 and 287.5 eV. The low BE component is assigned to adventitious carbon and methylene segments in the chaperone−substrate complex, whereas the high BE component at 287.5 eV is characteristic of carbon in carboxylic acid groups (*34*) and clearly is from the protein complex. When Ca^{2+} was present in the complex (Figure 8B), the BE of the carboxylate group shifted to 289.5 eV, a 2 nm shift, indicating a change in its microenviroment. This change in the BE of the surface-exposed carboxylate groups can be attributed to the binding of Ca^{2+} ion at or near these groups. Figure 8C shows the N 1s core level spectrum derived from the protein complex, where a single peak centered at 400.6 eV is observed. This BE arises from the nitrogens of the amino acids in the proteins (*35*) and therefore confirms the integrity of the protein structure in the complex. The most important Ca 2p spin−orbit components are shown in Figure 8D, which provides the useful information regarding the chaperone−substrate interactions. The Ca $2p_{3/2}$ core level BE is 347.5 eV and agrees well with the values of calcium in the +2 oxidation state, whereas the other BE is from the Ca $2p_{1/2}$ core level. It can clearly be seen that there is just one chemically distinct Ca^{2+} species suggesting a single chemical environment for these ions in the complex indicating the probable specific binding sites/pockets of Ca^{2+} ions in the chaperone. XPS measurements of Ca^{2+} binding to the chaperone only revealed similar results (data not shown), indicating that the changes observed are due to the conformational changes induced in the chaperone. XPS measurements were also carried out on the native HIV-1 PR in the absence of the chaperone, where the Ca^{2+} signal was below detection limits. These experiments clearly give the direct evidence of the putative Ca^{2+}-binding pockets in α-crystallin and also reveal the importance of the topographical changes induced in the chaperone in assisting the renaturation and release of active HIV-1 PR.

DISCUSSION

It has been well-established that conformational changes of folding intermediates play a major role in the binding and discharge of the substrate from molecular chaperones. Therefore, enormous efforts have been expended to study the conformational states of folding intermediates to decipher the molecular mechanisms of chaperone−substrate interactions. The chaperone−substrate interaction appears to be nonspecific with respect to the substrate proteins but specific in terms of the conformational states of the substrate (*36*). One of the signals for inducing such structural changes is the hydrolysis of ATP in case of DnaK (*37*) and GroEL (*38*). However, chaperones GroES (*39*) and BiP (*40*) do not require ATP hydrolysis, and instead, binding of the adenine nucleotide induces typological change in the chaperone. Although there is evidence that ATP enhances the function of α-crystallin as a molecular chaperone, and the role of ATP hydrolysis during the chaperone function of α-crystallin has not been clear (*41*). The α-crystallins are demonstrated to bind to the MG state of various proteins (*42*); however, the topographical changes and the signals inducing the release of the substrate during the chaperone function has not been addressed. This has been partly due to the nonavailability

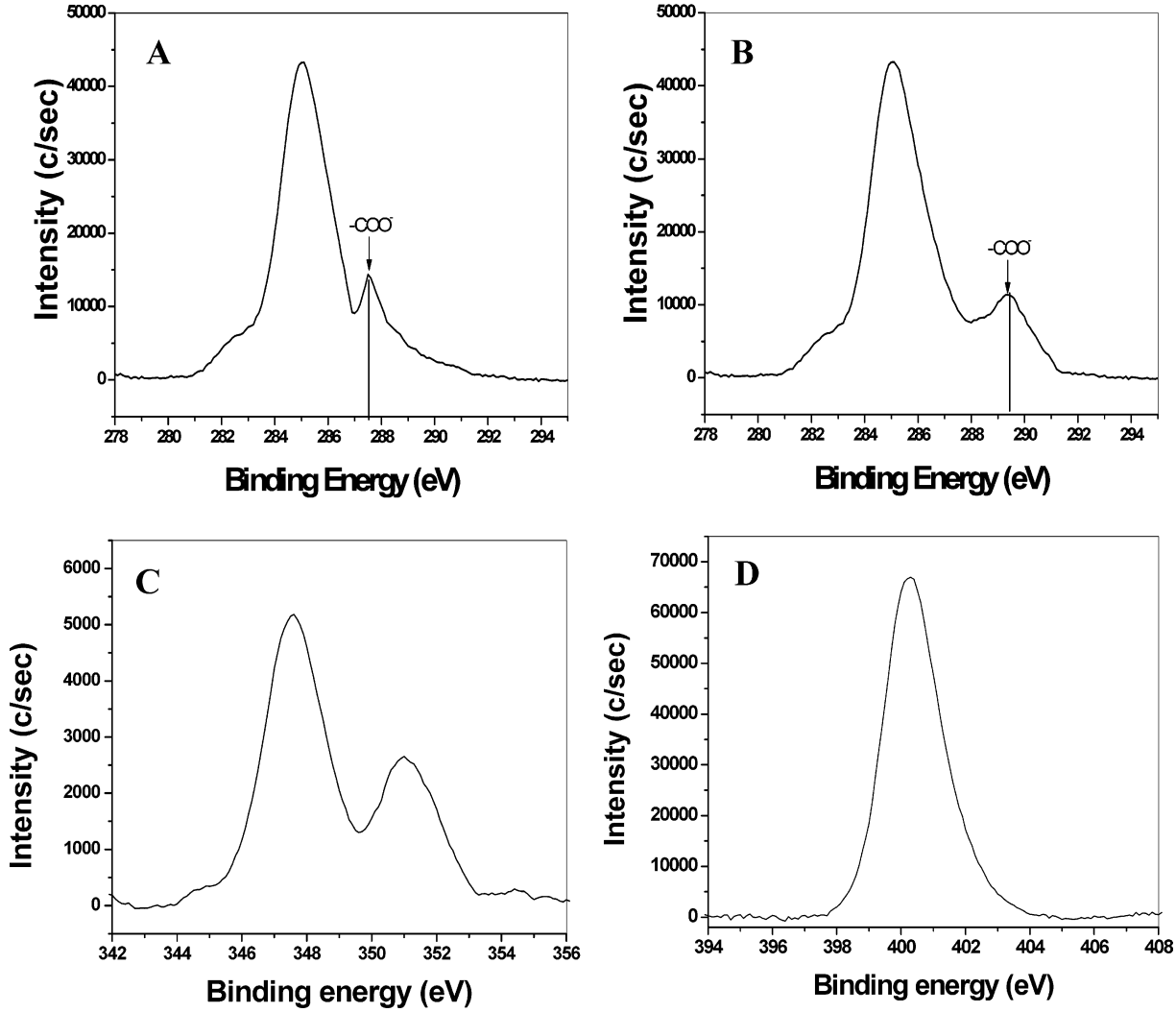

FIGURE 8: X-ray photoelectron spectroscopic analysis of the chaperone−substrate interaction. Binding of calcium to α-crystallin−HIV-1 PR−MG was monitored by XPS. (A) Core level spectra of C 1s in the absence of Ca^{2+} ions showed two peaks at BEs of 285 and 287.5 eV. The low BE is assigned to adventitious carbon and methylene segments, whereas the high BE component at 287.5 eV is characteristic of carbon in carboxylic acid groups. (B) In the presence of Ca^{2+} ions, the high BE peak shifted to 289.5 eV, indicating a change in its microenviroment, whereas the low BE remained unchanged. (C) N 1s core level spectrum indicated a single peak centered at 400.6 eV arising from the nitrogens of the amino acids of the protein complex. (D) Ca $2p_{3/2}$ core level BE is 347.5 eV. This value agrees well with the values of calcium in the +2 oxidation state and revealed the binding of Ca^{2+} ion to the chaperone−substrate complex, whereas the Ca $2p_{1/2}$ core level BE is 351 eV.

of the X-ray structure of α-crystallin, because of the polydisperse size distribution of both the natural and recombinant protein (*41*). In an attempt to investigate the topological changes and the signals essential for the release of the substrate protein from the chaperone−substrate complex of α-crystallin, we have used HIV-1 PR as a model substrate protein.

In the Gag-Pol polyprotein of HIV-1, the 99 amino acid PR is flanked at its N terminus by a transframe region (TFR) composed of the transframe octapeptide (TFP) and 48 amino acids of the p6pol, separated by a PR cleavage site. The intact precursor (TFP-p6pol-PR) has very low dimer stability and exhibits negligible levels of stable tertiary structure. Thus, the TFR functions by destabilizing the native structure, unlike proregions found in zymogen forms of monomeric aspartic PRs (*43*). Transient dimer formation leads to intramolecular autocatalytic cleavage first at the N terminus of the PR (p6pol/PR site), concomitant with stable structure formation and the appearance of enzymatic activity (*44*). Subsequent cleavage at the C terminus [PR/reverse transcriptase (RT) site] of the PR occurs via an intermolecular process. During the maturation of HIV-1 PR, an intermediate is present, which is more sensitive toward urea and acid denaturation than the mature PR because of the major interactions between the two subunits of the mature PR in the region of the N- and C-terminal strands (*45*). Although the kinetic and X-ray crystallographic studies have helped in understanding a great detail about the functional and structural aspects of the enzyme, the unfolding and folding pathways of HIV-1 PR still remain unexplored. From a number of NMR parameters determined under conditions of guanidine denaturation, the early folding nuclei have been identified, which include native as well as non-native secondary structures (*30*−*31*, *46*−*47*). Our understanding of the folding pathway of HIV-1 PR has been further strengthened by molecular modeling analysis (*32*); however, the stages through which the enzyme folds to its native conformation and the biochemical characterization of such states remains elusive.

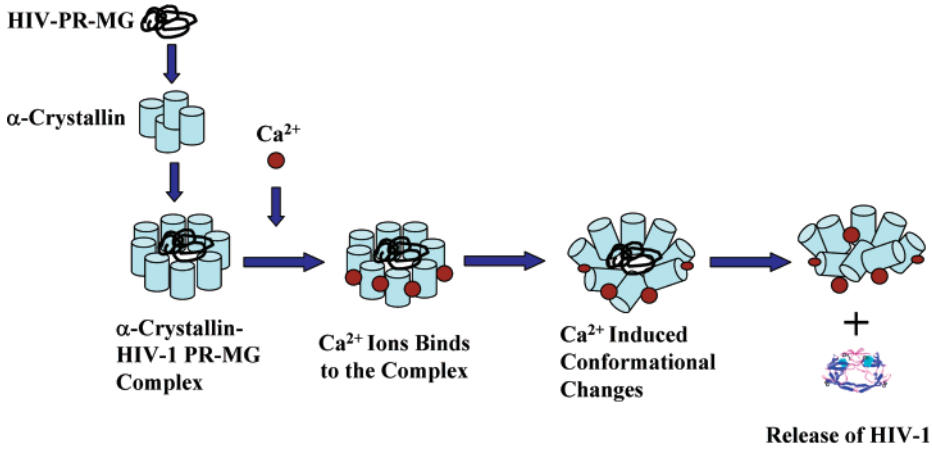

FIGURE 9: Schematic representation of the proposed mechanism of Ca^{2+} ion binding to the chaperone−substrate complex and release of the substrate protein. The HIV-1 PR−MG was rescued by α-crystallin because of its ability to prevent aggregation of the unfolded proteins; however, there was no regaining of the enzymatic activity. We visualize that HIV-1 PR refolds when it is bound to the chaperone; however, it was unable to get released from the chaperone complex. Our XPS and fluorescence data revealed that Ca^{2+} ions interact with the chaperone and induce localized conformational changes that are responsible for the release of the substrate protein. We propose that Ca^{2+} ions binds at or near the microenvironment of the acidic amino acids of the α-crystallin and change the hydrophobic interaction between the chaperone and substrate. These changes in the hydrophobic interactions may be sufficient to bring conformational changes in the chaperone responsible for the release of the active enzyme.

In this paper, we discuss the recent findings on the folding intermediates of HIV-1 PR and also focus on the calcium-binding properties of the molecular chaperone α-crystallin.

The tertiary structure of HIV-1 PR collapsed in the presence of GdnHCl in a concentration-dependent manner and unfolded completely at 8 M GdnHCl. HIV-1 PR lacked the ability to refold to the active form when unfolded at or above 3 M GdnHCl in the absence or presence of the chaperone and metal ion. However, at 2 M GdnHCl, HIV-1 PR retained the ability to refold and reconstitute to the active form in the presence of the chaperone and Ca^{2+}. Fluorescence and CD spectra revealed at 2 M GdnHCl that the tertiary structure differs from the native enzyme but substantial secondary structure is retained. The change in the near-UV CD provides information on the changes in the tertiary structural packing of the protein, whereas the changes in the far-UV CD report on the changes in the secondary structure. On the basis of these results, the intermediate observed at 2 M GdnHCl exhibits largely decreased tertiary structural packing with significant secondary structural elements. ANS, a hydrophobic fluorophore widely used to detect the exposed hydrophobic surfaces on the MG-like intermediates of several proteins (*42*) has been utilized to detect the MG state in the folding pathway of this enzyme. A maximum increase in the ANS fluorescence was observed when the protein was unfolded at 2 M GdnHCl, indicating the optimum exposure of hydrophobic surfaces. A comparison of our fluorescence and CD results with the ANS-binding studies points to the existence of a partially unfolded state around 2 M GdnHCl, which has the characteristics of a MG. The MG state is characterized to be as compact as the native protein with solvent-accessible hydrophobic regions and an appreciable amount of secondary structure with labile tertiary structure. Therefore, we believe that HIV-1 PR unfolds through an intermediate, which resembles the MG state. The binding of α-crystallin to the HIV-1 PR−MG suppressed aggregation of HIV-1 PR−MG and actively participated in the refolding and reactivation of HIV-1 PR in the presence of Ca^{2+}. The ability of the chaperone to rescue only the MG state and not the unfolded/misfolded protein can be attributed to the key role of hydrophobic interactions in the chaperone activity of α-crystallin. This corroborates the NMR data, where it was reported that hydrophobic interactions between the side chains may be important in driving the folding process of HIV-1 PR. Because the completely unfolded proteins lack the critical hydrophobic pockets essential for the binding of the chaperone, addition of Ca^{2+} ions cannot facilitate binding of α-crystallin to the unfolded proteins. Gel-filtration analysis further corroborated the formation of the chaperone−substrate complex and the release of HIV-1 PR from the complex because of the interaction of Ca^{2+} ions.

To decipher the molecular mechanism of the metal ion binding to the chaperone and its role in the substrate protein release, we have carried out XPS. XPS is based on the characteristic BE associated with the core atomic orbital of each element and is useful to identify the oxidation states and ligands of an atom. The role of the concerted effect of the Ca^{2+} and α-crystallin on the reconstitution of HIV-1 PR can be addressed by the results obtained from the XPS analysis. The shift in the BE of the surface-exposed carboxylate groups on the C 1s atomic spectrum of the chaperone−substrate complex in the presence of Ca^{2+} revealed that the metal ions bind at or near the microenvironment of acidic amino acids of the chaperone. The binding of Ca^{2+} to α-crystallin/α-crystallin−HIV-1 PR−MG induced localized conformational changes in the chaperone, which were reinforced by monitoring the Trp fluorescence of the chaperone. Addition of Ca^{2+} ions resulted in the decrease in the fluorescence intensity, which can be attributed to a change in the microenvironment of Trp residues α-crystallin, whereas a red shift in the emission maxima indicated gross conformational changes in the chaperone. It is previously reported that binding of Ca^{2+} ions results in the exposure of hydrophobic surfaces (*25*). We hypothesize that the binding of Ca^{2+} ions to the acidic microenvironment induces an electrostatic imbalance in the chaperone. This electrostatic imbalance interferes with the hydrophobic interactions, which are essential for the stabilization of the

chaperone−substrate interactions. A higher concentration of Ca^{2+} ion is known to induce aggregation because of the interaction with the exposed hydrophobic surfaces α-crystallin; however, at lower concentrations, the effect of the metal ion is to induce gross conformational changes, which are not substantial to induce aggregation of the chaperone. Therefore, it is important to point out that the concentration of Ca^{2+} ions plays a critical role in the reconstitution of HIV-1 PR. This is in accordance with the effect of the Ca^{2+} concentration to modulate the quality and efficiency of protein folding by calreticulin, a major Ca^{2+}-binding (storage) chaperone in the endoplasmic reticulum (*48*). Evidently, the presence of Ca^{2+} ions is not essential for the formation of the chaperone−substrate complex; it is clear that native α-crystallin possesses the critical hydrophobic pockets for the binding of the substrate protein. Therefore, further exposure of hydrophobic surfaces by metal ion binding may not facilitate its chaperone activity but is essential for the release of HIV-1 PR. Because hydrophobic interactions play an important role for the chaperone-mediated refolding of the substrate protein and Ca^{2+} ions interfere in the hydrophobic interactions, we visualize that the conformational changes induced in α-crystallin by the metal ion binding are responsible for the reconstitution of HIV-1 PR (Figure 9).

Calcium-binding proteins are known to have the characteristic EF hand or lipocortin- or annexin-like domains. There are proteins that have putative calcium-binding sites without the well-characterized binding domain called "orphan" motifs (*49*). Because the crystallographic structure of α-crystallin is not available and there has been no evidence of the calcium-binding motif in the protein, we are not able to pinpoint the exact binding site of the metal ion on the chaperone. However, with the existing XPS data, we propose a probable binding site/pocket at or near the exposed acidic amino acid residue (aspartate/glutamate) microenvironments of α-crystallin. In conclusion, we have detected a MG state in the folding pathway of HIV-1 PR and successfully reconstituted the active protein in the presence of α-crystallin and calcium.

REFERENCES

1. Gething, M. J., and Sambrook, J. (1992) Protein folding in the cell, *Nature 355*, 33−45.
2. Hartl, F. U. (1996) Molecular chaperones in cellular protein folding, *Nature 381*, 571−580.
3. Langer, T., Lu, C., Echols, H., Flanagan, J., Hayer, M. K., and Hartl, F. U. (1992) Successive action of DnaK, DnaJ, and GroEL along the pathway of chaperone-mediated protein folding, *Nature 356*, 683−689.
4. Celet, B., Akman-Demir, G., Serdaroglu, P., Yentur, S. P., Tasci, B., van Noort, J. M., Eraksoy, M., and Saruhan-Direskeneli, G. (2002) Anti-αB-crystallin immunoreactivity in inflammatory nervous system diseases, *J. Neurol. 247*, 935−939.
5. Renkawek, K., Voorter, C. E., Bosman, G. J., van Workum, F. P., and de Jong, W. W. (1994) Expression of αB-crystallin in Alzheimer's disease, *Acta Neuropathol. 87*, 155−160.
6. Vicart, P., Caron, A., Guicheney, P., Li, Z., Prevost, M. C, Faure, A., Chateau, D., Chapon, F., Tome, F., Dupret, J. M., Paulin, D., and Fardeau, M. (1998) A missense mutation in the αB-crystallin chaperone gene causes a desmin-related myopathy, *Nat. Genet. 20*, 92−95.
7. Arrigo, A. P., and Landry, J. (1994) In *The Biology of Heat Shock Proteins and Molecular Chaperones* (Morimoto, R. I. Ed.) pp 335−373, Cold Spring Harbor Laboratory Press, Cold Spring Harbor, New York.
8. Klemenz, R., Froeli, E., Steiger, R. H., Schaefer, R., and Aoyama, A. (1991) αB-Crystallin is a small heat shock protein, *Proc. Natl. Acad. Sci. U.S.A. 88*, 3652−3656.
9. Jakob, U., Gaestel, M., Engel, K., and Buchner, J. (1993) Small heat shock proteins are molecular chaperones, *J. Biol. Chem. 268*, 1517−1520.
10. Derham, B. K., and Harding, J. J. (1999) α-Crystallin as a molecular chaperone, *Prog. Retinal Eye Res. 18*, 463−509.
11. de Jong, W. W., Caspers, G. J., and Leunissen, J. A. M. (1998) Genealogy of the a-crystallin−Small heat-shock protein superfamily, *Int. J. Biol. Macromol. 22*, 151−162.
12. Kelley, M. J., David, L., Iwasaki, N., Wright, J., and Shearer, T. R. (1993) α-Crystallin chaperone activity is reduced by calpain II *in vitro* and in selenite cataract, *J. Biol. Chem. 268*, 18844−18849.
13. Horwitz, J. (1992) α-Crystallin can function as a molecular chaperone, *Proc. Natl. Acad. Sci. U.S.A. 89*, 10449−10453.
14. Jakob, U., and Buchner, J. (1994) Assisting spontaneity: The role of Hsp90 and small Hsps as molecular chaperones, *Trends Biochem. Sci. 19*, 205−211.
15. van den Ijssel, P., Norman, D. G., and Quinlan, R. A. (1999) Molecular chaperones: Small heat shock proteins in the limelight, *Curr. Biol. 11*, R103−R105.
16. Narberhaus, F. (2002) α-Crystallin-type heat shock proteins: Socializing minichaperones in the context of a multichaperone network, *Microbiol. Mol. Biol. Rev. 66*, 64−93.
17. Muchowski, P. J., and Clark, J. L. (1998) ATP-enhanced molecular chaperone functions of the small heat shock protein human α-B crystalline, *Proc. Natl. Acad. Sci. U.S.A. 95*, 1004−1009.
18. Nath, D., Rawal, U., Anish, R., and Rao, M. (2002) α-Crystallin and ATP fecilitate the *in vitro* renaturation of xylanase: Enhancement of refolding by metal ions, *Protein Sci. 11*, 2727−2734.
19. Wang, K. and Spector, A. (2000) α-Crystallin prevents irreversible protein denaturation and acts cooperatively with other heat-shock proteins to renature the stabilized partially denatured protein in an ATP-dependent manner, *Eur. J. Biochem. 267*, 4705−4712.
20. Avilov, S. V., Aleksandrov, N. A., and Demchenko, A. P. (2004) Quaternary structure of α-crystallin is necessary for the binding of unfolded proteins: A surface plasmon resonance study, *Protein Pept. Lett. 1*, 141−148.
21. Regini, J. W., Grossmann, J. G., Burgio, M. R., Malik, N. S., Koretz, J. F., Hodson, S. A., and Elliott, G. F. (2004) Structural changes in α-crystallin and whole eye lens during heating, observed by low-angle X-ray diffraction, *J. Mol. Biol. 336*, 1185−1194.
22. Spector, A., Adams, D., and Krul, K. (1974) Calcium and high molecular weight protein aggregates in bovine and human lens, *Invest. Opthalmol. Visual Sci. 13*, 982−990.
23. Jedzaniak, J. A., Kinoshita, J. H., Yates, E., Hocker, I., and Benedek, G. B. (1973) Calcium-induced aggregation of bovine lens α crystallins, *Invest. Opthalmol. Visual Sci. 11*, 905−915.
24. Hawse, J. R., Cumming, J. R., Oppermann, B., Sheets, N. L., Reddy, V. N., and Kantorow, M. (2003) Activation of metallothioneins and α-crystallin/sHSPs in human lens epithelial cells by specific metals and the metal content of aging clear human lenses, *Invest. Ophthalmol. Visual Sci. 44*, 672−679.
25. del Valle, L. J., Escribano, C., Perez, J. J., and Garriga, P. (2002) Calcium-induced decrease of the thermal stability and chaperone activity of α-crystallin, *Biochim. Biophys. Acta 1601*, 100−109.
26. Dunn, B. M., Gutchisna, A., Wlodawer, A., and Kay, J. (1993) Subsite preferences of retroviral proteinases, *Methods Enzymol. 241*, 254−278.
27. Yamazaki, T., Nicholson, L. K., Torchia, D. A., Stahl, S. J., Kaufman, J. D., Wingfield, P. T., Domaille, P. J., and Campbell-Burk, S. (1994) Secondary structure and signal assignments of human-immunodeficiency-virus-1 protease complexed to a novel, structure-based inhibitor, *Eur. J. Biochem. 219*, 707−712.
28. Freedberg, D. I., Wang, Y., Stahl, S. J., Kaufman, J. D., Wingfield, P. T., Kiso, Y., and Tochia, D. A. (1998) Flexibility and function in HIV protease: Dynamics of the HIV-1 protease bound to the asymmetric inhibitor kynostatin 272 (KNI-272), *J. Am. Chem. Soc. 120*, 7916−7923.
29. Panchal, S. C., Pillai, B., Hosur, M. V., and Hosur R. V. (2000) *Curr. Sci. 79*, 1684−1695.
30. Bhavesh, N. S., Panchal, S. C., Mittal, R., and Hosur, R. V. (2001) NMR identification of local structural preferences in HIV-1 protease tethered heterodimer in 6 M guanidine hydrochloride, *FEBS Lett. 509*, 218−224.

31. Bhavesh, N. S., Sinha, R., KrishnaMohan, P. M., and Hosur, R. V. (2003) NMR elucidation of early folding hierarchy in HIV-1 protease, *J. Biol. Chem. 278*, 19980−19985.
32. Levy, Y., Caflisch, A., Onuchic, J. N., and Wolynes, P. G. (2004) The folding and dimerization of HIV-1 protease: Evidence for a stable monomer from simulations, *J. Mol. Biol. 340*, 67−79.
33. Dash, C., and Rao, M. (2001) Interactions of a novel inhibitor from an extremophilc *Bacillus* sp with HIV-1 protease: Implications in mechanism of inactivation, *J. Biol. Chem. 276*, 2487−2493.
34. Sastry, M., and Ganguly, P. (1998) Determination of C 1s core level chemical shifts in some Langmuir−Blodgett films using a modified Sanderson formalism, *J. Phys. Chem. A 102*, 697−702.
35. Gole, A., Dash, C., Mandale, A. B., Rao, M., and Sastry, M. (2000) Fabrication, characterization, and enzymatic activity of encapsulated fungal protease-fatty lipid biocomposite films, *Anal. Chem. 72*, 4301−4309.
36. Martin, J., and Hartl, F. U. (1997) Chaperone-assisted protein folding, *Curr. Opin. Struct. Biol. 7*, 41−52.
37. Mayer, M. P., Rüdiger, S., and Bukau, B. (2000) Molecular basis for interactions of the DnaK chaperone with substrates, *Biol. Chem. 381*, 877−885.
38. Mendozza, J. A., Rogers, E., Lorimer, G. H., and Horowitz, P. M. (1991) Chaperonins facilitate the *in vitro* folding of monomeric mitochondrial rhodanese, *J. Biol. Chem. 266*, 13044−13049.
39. Schmidt, M., and Buchner, J. (1992) Interaction of GroE with an all-β-protein, *J. Biol. Chem. 267*, 16829−16833.
40. Kassenbrock, C. K., and Kelly, R. B. (1989) Interaction of heavy chain binding protein (BiP/GRP78) with adenine nucleotides, *EMBO J. 8*, 1461−1467.
41. Jaenicke, R., and Slingsby, C. (2001) Lens crystallins and their microbial homologs: Structure, stability, and function, *Crit. Rev. Biochem. Mol. Biol. 36*, 435−499.
42. Rawat, U., and Rao, M. (1998) Interactions of chaperone-crystallin with the molten globule state of xylose reductase. Implications for reconstitution of the active enzyme, *J. Biol. Chem. 273*, 9415−9423.
43. Louis, J. M., Marius-Clore, G., and Gronenborn, A. M. (1999) Autoprocessing of HIV-1 protease is tightly coupled to protein folding, *Nat. Struct. Biol. 6*, 868−875.
44. Louis, J. M., Wondrak, E. M., Kimmel, A. R., Wingfield, P. T., and Nashed, N. T. (1999) Proteolytic processing of HIV-1 protease precursor, kinetics, and mechanism, *J. Biol. Chem. 274*, 23437−23442.
45. Wondrak, E. M., Nashed, N. T., Haber, M. T., Jerina, D. M., and Louis, J. M. (1996) A transient precursor of the HIV-1 protease. Isolation, characterization, and kinetics of maturation, *J. Biol. Chem. 271*, 4477−4481.
46. Ishima, R., Ghirlando, R., Tozser, J., Gronenborn, A. M., Torchia, D. A., and Louis, J. M. (2001) Folded monomers of HIV-1 protease, *J. Biol. Chem. 276*, 49110−49116.
47. Ishima, R., Torchia, D. A., Lynch, S. M., Gronenborn, A. M., and Louis, J. M. (2003) Solution structure of the mature HIV-1 protease monomer: Insight into the tertiary fold and stability of a precursor, *J. Biol. Chem. 278*, 43311−43319.
48. Rajani, B., Shridas, P., Sundari, C. S., Muralidhar, D., Chandani, S., Thomas, F. and Sharma, Y. (2001) Calcium binding properties of γ-crystallin: Calcium ion binds at the key $\beta\gamma$-crystallin fold, *J. Biol. Chem. 276*, 38464−38471.
49. Michalak, M., Robert-Parker, J. M., and Opas, M. (2002) Ca^{2+} signaling and calcium binding chaperones of the endoplasmic reticulum, *Cell Calcium 32*, 269−278.
50. Shirley, D. A. (1972) High-resolution X-ray photoemission spectrum of the valence bands of gold, *Phys. Rev. B: Condens. Matter Mater. Phys. 5*, 4709−4714.

BI048378N